

Computation of the Aerodynamic Forces, Design and Development of an Orinthopter

Nishanth P¹, Haseebuddin M R², Pranav Srinath¹, Naba Saleel¹, Pannaga Hegde¹ and Mohan Das A N³

¹UG Scholar, Department of Mechanical Engineering, Dayananda Sagar College of Engineering, Bengaluru, India. Email: pnishanth31@gmail.com

²Associate Professor, Department of Mechanical Engineering, Dayananda Sagar College of Engineering, Bengaluru, India. Email: haseebdsce@gmail.com

³Assistant Professor, Department of Mechanical Engineering, Dayananda Sagar College of Engineering, Bengaluru, India. Email: mohandasakkur@gmail.com

Abstract

An aircraft flying by flapping its wings is called as ornithopter. Ornithopters are called as flapping-wing models and usually built to the size of birds. The wings of the ornithopter generate lift as well as thrust. For the low Reynolds number range, flapping wings are the most efficient means of propulsion, which is why a lot of MAVs (micro aerial vehicles) have flapping wings. They also have the added advantage of better manoeuvrability, as natural flyers such as birds and insects that demonstrate superior flight skills. Ornithopters are used for military applications such as aerial reconnaissance and animal behavioural research since they are made to resemble birds.

The present work focuses on the computation of the aerodynamic forces, design and fabrication of an ornithopter. A code is developed to compute the lift, thrust and drag forces generated by the wings using a theoretical model of equations. The design proposed in this study uses a transverse shaft gear system for the power train mechanism to flap the wings. The model was tested and optimizations were done for improving the flight.

Keywords: Aerodynamic forces, ornithopter, micro aerial vehicles, flapping-wing model.

1.0 Introduction

Ornithopters are flapping-wing aircraft that generate the lift and thrust required for flight by flapping their wings. Although this has much relevance to how flight is achieved in nature, this method has been largely replaced by fixed-wing aircraft in the airline industry. This owes to the complexities involved in its design and its kinematics.

Lippisch in 1929 proposed to make human-powered ornithopters and hired a pilot to fly his models [1]. It is observed during the experiments that flapping a stiff wing did not produce any forward

thrust, even after changing the incidence angle. Also a flexible trailing edge for the wing is implemented which leads to massive difference in the propulsive action. R T Jones worked on the ornithopter wing to find a method for flapping with minimum energy [2]. This work gives primary importance to the bending moment on the wing root and tried to minimize the induced drag for a periodically varying bending moment on the wing root. Importance is given to find the load distribution that minimizes vortex drag for a given bending moment. In this work, it has been suggested that counter flapping wings would be a good alternative for ornithopters, which consist of

wings in tandem moving in opposite phases. DeLaurier [3] used a double surface airfoil and studied its performance and conducted various analyses to conclude that it was practical to use this design which had a constant semi-span simple harmonic flapping and the pitching was solely due to the aeroelastic response due to this.

A research performed in Singapore studied three different wings, with different structure and different materials to observe their performance and understand their behaviour [4]. They conducted analyses on Ansys, designed and fabricated these to test them out experimentally. Among these 3 wings, they found that the best alternative out of them was a flat wing made with a material called orcan, flapping at medium frequency. In M Afzaal Malik and Farooq Ahmad's article on the effect of design parameters of lift, thrust and drag of ornithopter [5]. In this work the relation between the different design parameters and the forces produced by the flapping of the wings of said dimensions are calculated analytically. J.D. DeLaurier and J.M. [6] experimentally tried to calculate the relation between average thrust coefficient and frequency for different flap angle. They used a rectangular planform of an 8-inch span and a 2-inch chord. Studies concluded that as pitch amplitude increases thrust coefficient increases. This work concluded that leading- edge suction is also important for thrust production. K.D. Jones and M.F. Platzer [7] developed a model using numerical methods that would predict the pitch amplitude. They mentioned that if the pitch amplitude exceeded the angle of attack, the drag effect was increased profoundly and thus the pitch amplitude should be maintained less than the angle of attack for optimal power consumption. In an article 'Computational Fluid Dynamics of a Flapping Wing Under Prescribed Motion' [8], Xavier performs a CFD analysis on a flapping wing using ANSYS fluent. The model was subsequently validated against the experimental results and found to provide very similar values. It was then compared to a rigid wing model under identical conditions. It was found that the flexible wing generated much higher forces than a rigid wing at the same flapping frequency [9].

From the literature, studies reveal the influences of various equations to determine the forces on the bird and the sizing of the bird. In this paper, a python code is generated to determine the forces on the bird. Further, a method to calculate the number of gears and number of teeth on gears has been discussed. The model of the ornithopter is also built and the forces were measured experimentally and verified with the code.

2.0 Mathematical Model

Flapping wings have different motions in three axes as shown in Figure 1. Flapping is the up and down motion of the wing which generates most of the power. It also has the highest degree of freedom. The pitching motion which varies along the wingspan is called eathering. Also the Lead lag is the lateral movement of wing. However, for simplicity and convenience, most ornithopters just use flapping accompanied by natural pitching due to them being flexible to produce lift and thrust.

Flapping consists of upstroke and downstroke as shown in Figure 2. The resultant force during downstroke is angled forward and has lift and thrust as two components. The relative angle of attack (AOA) in upstroke is positive at the root but it can become negative while moving down to the tip of the wing. Hence, the inner region of the wing has a resultant force that is facing upwards but tilted backwards, therefore producing lift and drag during upstroke. The outer part

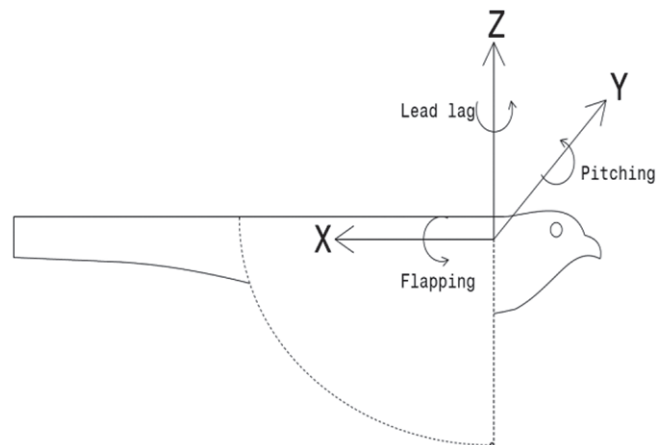


Figure 1: The three axes of flapping wing

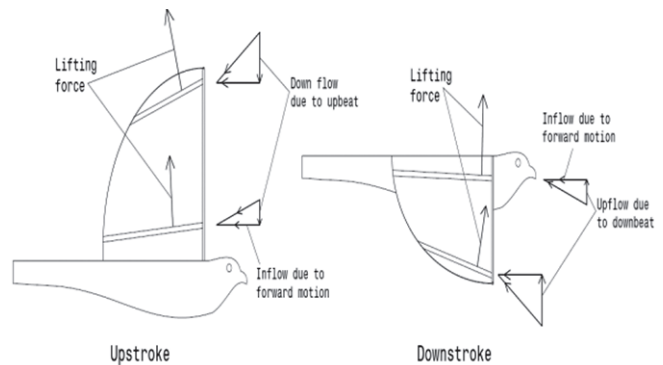


Figure 2: Upstroke and Downstroke

of the wing produces lift and drag or lift and thrust depending on whether the AOA is positive or negative.

This study aims to compute the forces generated through an analytical approach to flapping wing aerodynamics using an unsteady model. The quasi-steady model, which is another popular method, assumes low flapping frequencies and neglects the wake effects. However, this study uses a modified strip theory and Theodorsen's approach was modified by Jones which considers the unsteady wake characteristics.

The assumptions made for this approach are:

- The wings are flexible and have a rigid leading edge spar and the wing planform is semi-elliptical.
- The mechanism's drive train only produces flapping motion in the wings.
- The leading edge spar is a pivot about which the flexible wings can pitch due to aerodynamic or inertia loads.
- Attached airflow.
- Flapping and pitching motions are given by sinusoidal wave equations with some lag between them.

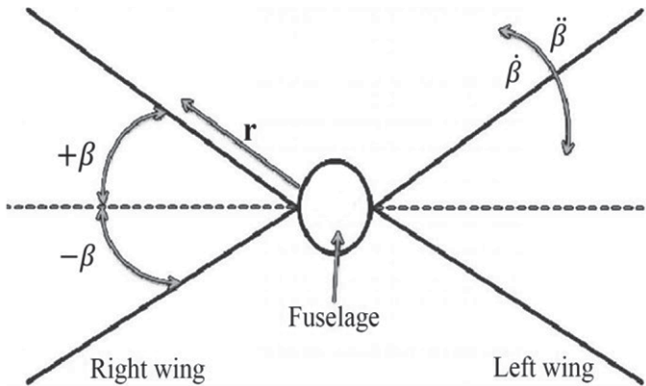


Figure 3: Flapping wing as seen from the front view

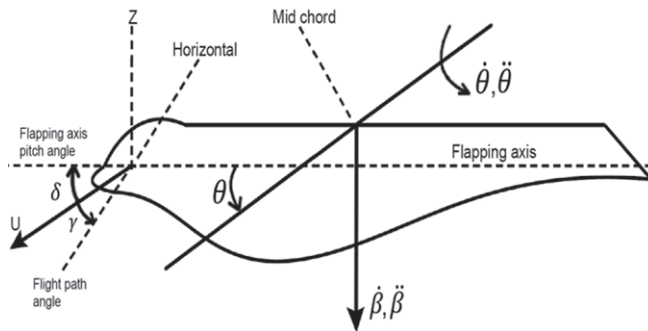


Figure 4: Kinematics of flapping wing

Flapping angle β as shown in Figure 3 is given by a sinusoidal wave function. Flapping angle β , flap rate and pitching angle θ shown in Figure 4 are given by

$$\beta(t) = \beta_{max} \cos(2\pi ft) \quad \dots (1)$$

$$\dot{\beta}(t) = -2\pi f \beta_{max} \sin(2\pi ft) \quad \dots (2)$$

$$\theta(t) = \frac{r}{B} \theta_o \cos(2\pi ft + \Phi) \quad \dots (3)$$

where θ – max pitch angle, Φ – pitching- flapping lag, r – distance along the wingspan at the given instant.

The two components of relative wind – horizontal (x) and vertical (z) velocities, as shown in Figure 5, are given by

$$V_x = U \cos \delta + (0.75 * c * \dot{\theta} * \sin \theta) \quad \dots (4)$$

$$V_z = U \sin \delta + (-r * \dot{\beta} * \cos \beta) + (0.75 * c * \dot{\theta} * \cos \beta) \quad \dots (5)$$

The relative wind velocity V , relative angle between the horizontal and vertical components ψ and the relative angle of attack α are given by

$$V = \sqrt{V_x^2 + V_z^2} \quad \dots (6)$$

$$\psi = \tan^{-1} \frac{V_z}{V_x} \quad \dots (7)$$

$$\alpha = \psi + \theta \quad \dots (8)$$

The sectional coefficient of lift because of circulation (Kutta-Joukowski condition, flat plate) is given by

$$C_{l-c} = 2\pi C(k) \sin \alpha \quad \dots (9)$$

where $C(k)$ – Theodorsen Lift Deficiency factor can be calculated as

$$C(k) = \sqrt{F^2 + G^2} \quad \dots (10)$$

$$F = 1 - \frac{C_1 \cdot k^2}{k^2 + C_2^2} \quad \dots (11)$$

$$G = - \frac{C_1 \cdot C_2 \cdot k}{k^2 + C_2^2} \quad \dots (12)$$

$$C_1 = \frac{0.5AR}{2.32 + AR} \quad \dots (13)$$

$$C_2 = 0.181 + \frac{0.772}{AR} \quad \dots (14)$$

The sectional lift dL_c is given by

$$dL_c = \frac{1}{2} \rho V^2 C_{l-c} * c * dr \quad \dots (15)$$

which is integrated along the wingspan to get the lift generated. Here, dr and c are width of the given wing

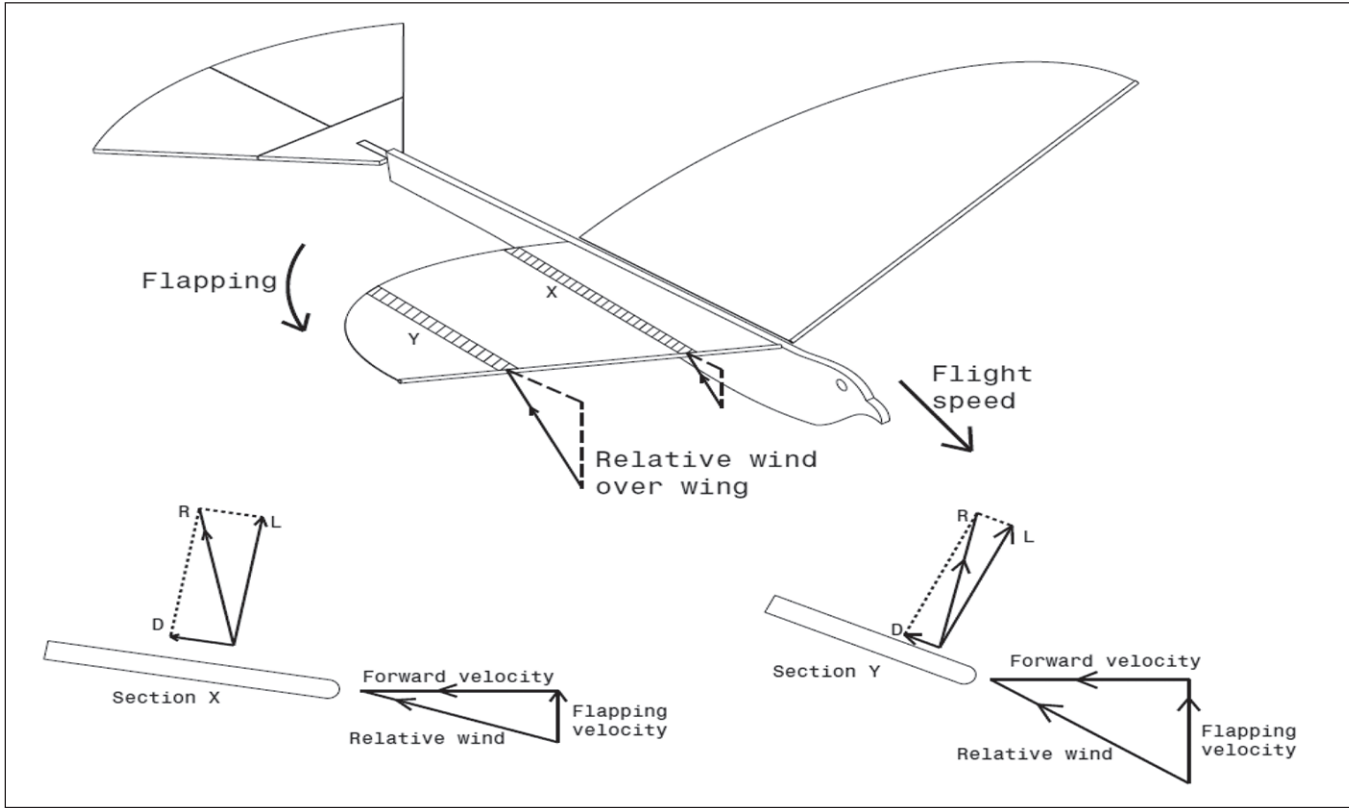


Figure 5: Relative airflow over the wings

element and chord length respectively. The momentum transferred to the wing from the accelerating air acts on the mid-chord in a direction perpendicular to the wing and is given by

$$dN_{nc} = -\frac{\rho\pi c^2}{4}(\dot{\theta}U + r\ddot{\beta} \cos \theta - 0.5\ddot{\theta})dr \quad \dots (16)$$

The drag force consists of profile drag dD_p and induced drag dD_i . These are given by

$$dD_p = \frac{1}{2}\rho V^2 C_{dp} * c * dr \quad \dots (17)$$

$$dD_i = \frac{1}{2}\rho V^2 C_{di} * c * dr \quad \dots (18)$$

where C_{dp} and C_{di} are profile drag and induced drag coefficients, and are given by

$$C_{dp} = K * C_f \quad \dots (19)$$

$$C_f = 0.445 (\log_{10} Re)^{-2.58} \quad \dots (20)$$

$$C_{di} = \frac{C_{l-c}^2}{e * \pi * AR} \quad \dots (21)$$

Where, C_f is the coefficient of skin friction for a flat

plate. The value of the factor K used to calculate profile drag was determined to be 4.4 by Scherer [14] and the same value is used in this study as well. C_{di} is the coefficient of induced drag, and e is the efficiency factor. For semielliptical wings the efficiency factor of the wing is 0.8. Total drag for the section is calculated using

$$dD_d = dD_p + dD_i \quad \dots (22)$$

Lift due to circulation dL_c , non-circulatory force dN_{nc} and drag force dD_d for every section of the wing varies at every instant. These forces resolved and the resulting vertical and horizontal components of the forces are

$$\begin{aligned} dF_{ver} &= (dL_c \cos \psi \cos \delta) \\ &+ (dN_{nc} \cos(-\theta) \cos \beta \cos \delta) \\ &+ (dD_d \sin \psi \cos \delta) \end{aligned} \quad \dots (23)$$

$$\begin{aligned} dF_{hor} &= (dL_c \sin \psi \cos \delta) \\ &+ (dN_{nc} \sin(-\theta) \cos \beta \cos \delta) \\ &- (dD_d \cos \psi \cos \delta) \end{aligned} \quad \dots (24)$$

These instantaneous forces integrated along the span and averaged to get the total average lift and thrust. If one flap cycle is divided into 'm' equal time

steps and the wing is divided into 'n' strips of equal width, then

$$\text{Average lift} = \frac{1}{m} \sum_{i=1}^n \sum_{j=0}^m dF_{ver} \quad \dots (25)$$

$$\begin{aligned} &\text{Average thrust} \\ &= \frac{1}{m} \sum_{i=1}^n \sum_{j=0}^m dF_{hor} \quad \dots (26) \end{aligned}$$

$$\text{Average drag} = \frac{1}{m} \sum_{i=1}^n \sum_{j=0}^m dD_d \quad \dots (27)$$

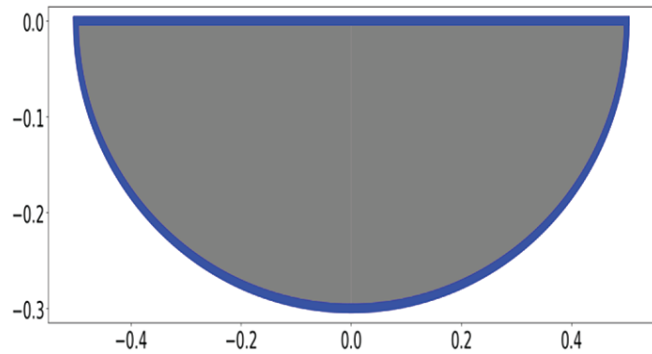


Figure 6: The wing considered for the code

2.1 Computation of Forces Using the Theoretical Model

The dimensions of the semi-elliptical wing used for the computation of forces are 1m span and 0.3m root chord, as shown in Figure 6. A code was written on

python to model the unsteady aerodynamics of flapping wings. The results were plotted as shown in Figure 7. The average lift, thrust and drag values over the cycle, when the flapping frequency is 7 flaps per sec, are tabulated in Table 1.

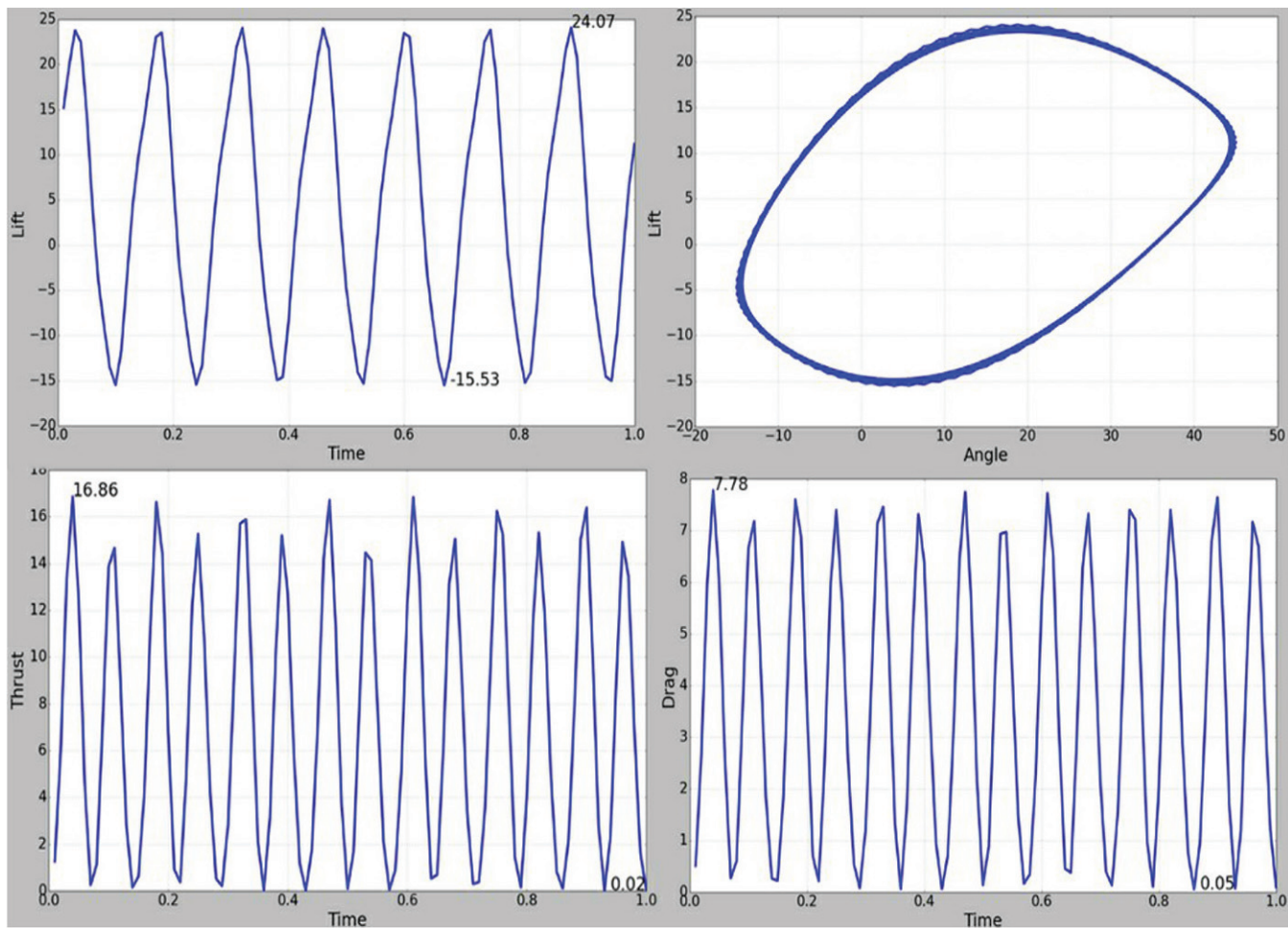


Figure 7: Various plots obtained from the code

Table 1: Results from theoretical model

Component	Force (in N)
Lift	4.301
Thrust	7.231
Drag	3.541

3.0 Design of Orinthopter

3.1 Gear Design

The gears were used to transfer the motion of the motors to the flapping wings with necessary reduction in its speed. This is a pivotal part of the flapping mechanism required in ornithopters. Involute gears were used for this purpose, however, the problem faced in using this was interference, which could be avoided by reducing the base circle/dedendum circle diameter, reducing the height of the gear teeth (undercutting of teeth) and increasing the number of teeth above the minimum number of teeth required (T_{min}). By reducing the base circle, the pressure angle increases. Due to the maximum pressure angle barrier of 25° , this option was not viable. Therefore to avoid interference we proposed to increase the number of teeth above T_{min} and undercutting. The gear reduction ratio was calculated as 21. A compound gear train was chosen for the flapping mechanism since it fills lateral space and a higher gear reduction ratio is possible with minimum space. A compound gear train with 2 simple gear trains was implemented with a pressure angle of 20° as it was found to be the optimal pressure angle for transmitting speed. The module of the mating gears was taken as 1 considering the law of gearing. If the module were to be kept more than 1 then the diameter of the gears would increase causing the gears to consume more space. If the module were to be kept less than 1 then, the gear tooth height will not be sufficient enough to operate at a higher work speed. In our model, required speed of 7rps is maintained to work at 50% of the speed of the motor. This was done to compensate for any external turbulence that may occur during the flight in the real world. So to prevent this turbulence the flap speed of the wings can be increased thereby compensating for the disturbance. The speed of the motor can be varied by using an ESC (Electronic Speed Controller). Due to this, the required gear reduction was reduced from 21 to 10.5.

The number of teeth in the driver gear is given by equation 28 and min number of teeth in pinion gear is given by equation 29. G is the gear reduction value and

θ is the pressure angle.

$$\begin{aligned}
 T &= \frac{2A_w}{\sqrt{1 + \frac{t}{T}(\frac{t}{T} + 2)(\sin \theta)^2 - 1}} \\
 &= \frac{2A_w}{\sqrt{1 + \frac{1}{G}(\frac{1}{G} + 2)(\sin \theta)^2 - 1}} \quad \dots (28)
 \end{aligned}$$

$$\begin{aligned}
 t &= \frac{2A_p}{\sqrt{1 + \frac{T}{t}(\frac{T}{t} + 2)(\sin \theta)^2 - 1}} \\
 &= \frac{2A_p}{\sqrt{1 + G(G + 2)(\sin \theta)^2 - 1}} \quad \dots (29)
 \end{aligned}$$

The addendum coefficient is the product of the fraction of module (f) and module (m). Since the teeth of the gear are stubbed, the value of f is 0.5 and the module remains the same.

$$A_w = f * m \quad (30)$$

Since in this model 2 simple gear trains are used for the specific gear train value for such mating gear. Thus, for Gears A and Gear B, the value of $G=3.5$. Thus, the minimum number of teeth for the driven gear was calculated to be 26.42 and the number of teeth of the driver gear is 35 and the number of teeth in pinion gear is 10.

Similarly, for Gears C and Gears D, the gear train value is 3. Implementing the value of G in the minimum number of teeth formula, we get the minimum number of teeth in driven gear to be equal to 22.47. Hence, the number of teeth on driver gear to be equal to 30.

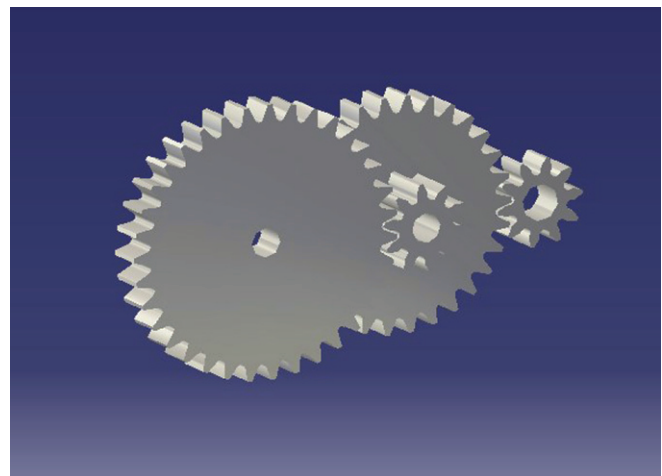


Figure 8: Model of the gear system named A, B, C, D (right to left)

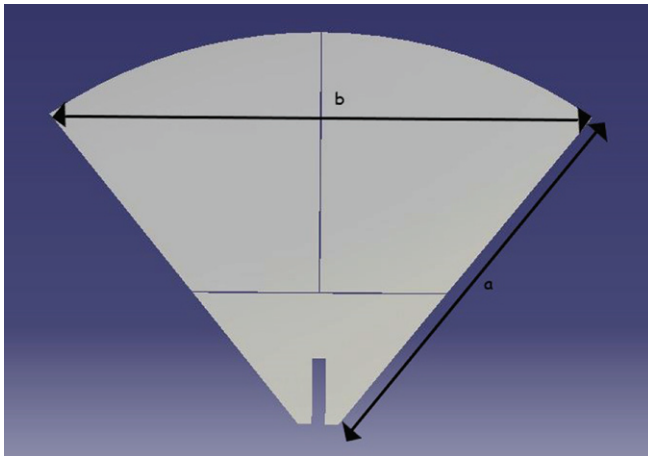


Figure 9: Triangular tail with dimensions marked

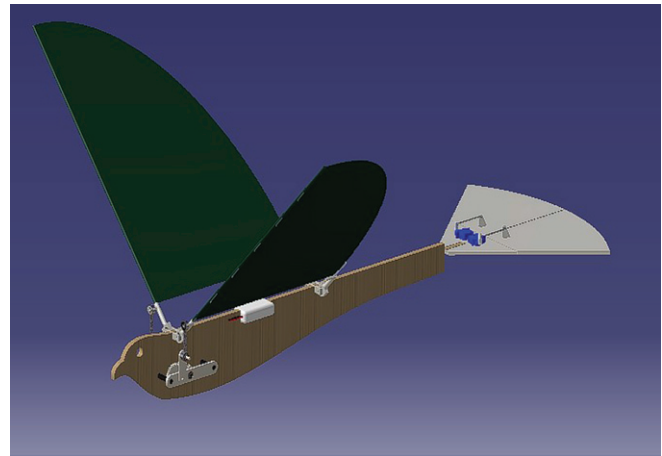


Figure 11: Isometric assembled view of the ornithopter

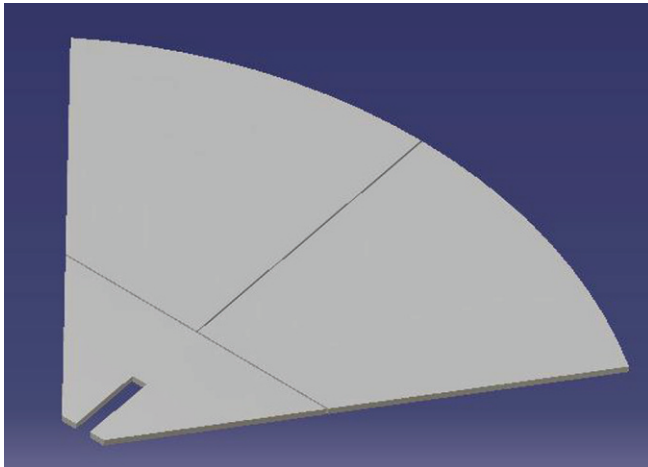


Figure 10: Isometric view of the tail

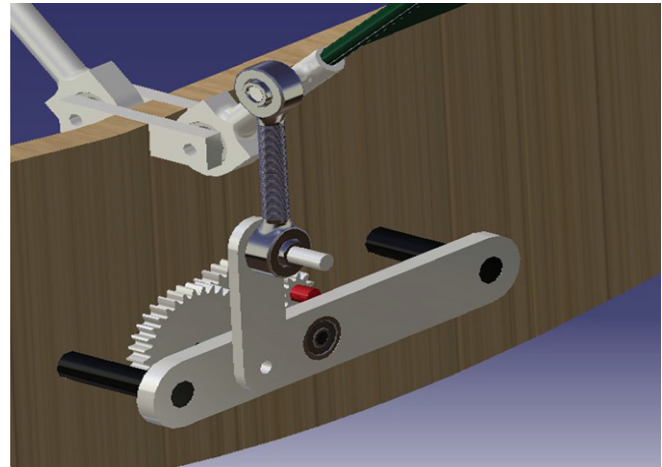


Figure 12: Close-up of the flapping mechanism

Corresponding to this the number of teeth on driver gear is 10. The reason it is chosen is just to make sure that the pinion gear (driver gear) to have at least 10mm of diameter to have good strength. Figure 8 shows the CAD image of the gear train—named A, B, C, D from right to left.

3.2 Tail Sizing

The tail is the most important component of the aircraft in terms of its stability and control. Various configurations of the tail are considered to finally arrive at the triangular wing design. This configuration had the most resemblance to the tails of birds and hence would make the model look less conspicuous. The initial problem faced is the effectiveness of the tail since the aerodynamics of an ornithopter is not identical to that of a fixed-wing aircraft due to the

flapping mechanism involved. However, the wake of the flapping wing exists throughout the wingspan, which means the tail has airflow over it, adding to its effectiveness in hover and slow flight. This allowed to go ahead with the design of the tail.

The tail arm calculated for the tail was 0.65m. The dimensions were:

- $a = 0.3\text{m}$
- $b = 0.4\text{m}$

where a and b are as marked in Figure 9.

3.3 Assembly of Ornithopter

All the connectors are assembled onto the fuselage and the 8mm rods are inserted into the supports as well as the fuselage. The wing rods are inserted into the wing connectors and a carbon fibre rod passes through the wing connector and the link which sits on

the fuselage. A similar connection is made at the rear end of the fuselage. The extension of the fuselage is inserted in the slot provided in the tail. The motors and gears are assembled onto the supports and shafts respectively. In order to achieve flapping, we had to use a rod-end bearing which can be seen in Figure 12. Figure 11 shows the assembled CAD model.

4.0 Fabrication of Orinthopter Parts

A feasible manufacturing process is followed aimed at reducing the cost of the model while ensuring that conforms to all the mission requirements. The materials were selected by considering their weight and the objective was to make the aircraft as light as

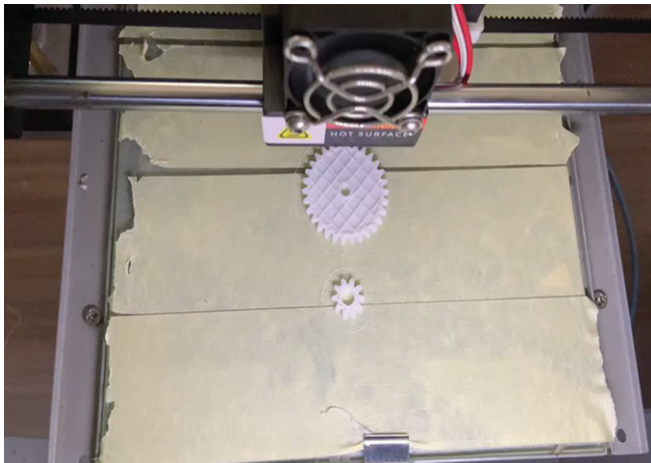


Figure 13: 3-D printing components of flapping mechanism and gears



Figure 14: The underside of the wing

possible while maintaining enough strength to withstand all the loads acting on it. The gears used in the design as well as various components used in the flapping mechanism was 3D printed using the material PLA. The 3D printer dimensions were 160mm x 160mm. We kept the bed temperature as 60°C and the nozzle temperature as 120°C. The flow percentage was 100 and the infill for most of the parts were set to 10%. The same for delicate parts such as the wing connector and the 7mm gear were set to 30%. The layer height was set to 1mm and there was 0.5mm tolerance given to all the holes in the design to make sure the complimentary part slides in easily. Figure 13 shows a picture of the gears being printed.

The wings are made out of covering film, which is a common material in fixed-wing aircraft. The wing has one main spar which is a 4mm carbon fibre rod and one cross spar which is a 3mm CF rod as shown in Figure 14. Two CF rods were used on both halves of the wing as fingers and this configuration gave the best results result for lift and drag. Figure 14 shows the bottom phase of the wing and Figure 15 shows the top phase of the wing.

Depron of 5mm thickness was used for manufacturing the tail. It was hand cut and it had a slot that facilitated easy assembly to the fuselage. Servos were used to move the control surfaces with the help of control horns as can be seen in Figure 16.

The fuselage was CNC cut out of balsa wood of thickness 5mm. Two of these cut-outs were joined together to make a fuselage of width 10mm. There were holes cut out with a clearance of 1mm to insert the gear shafts without interference. An extrusion was given at the rear end of the fuselage and a complimentary slot made on the tail so it could easily be fixed together. An 8mm hole was made on the



Figure 15: Top view of the wing



Figure 16: Tail



Figure 17: Gear assembly

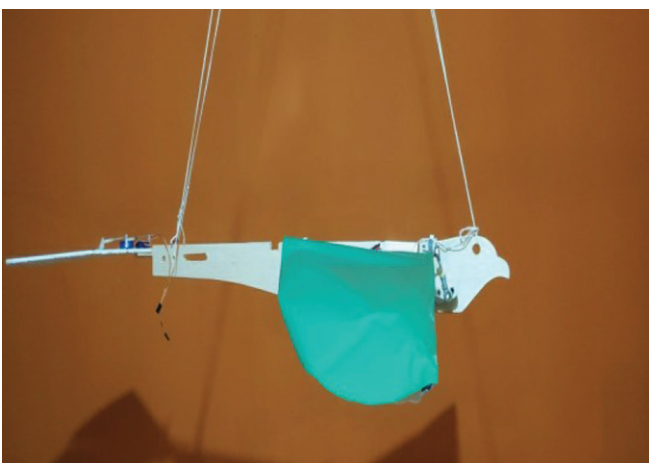


Figure 18: Full assembly of ornithopter

fuselage near the gear shafts. An 8mm CF rod was inserted into these holes which acted as supports for the motor and gear fixture.

All the parts were assembled in the end. Metlok 743 industrial grade single component instant bonding adhesive was used to glue the various parts together. The CF rods were inserted into the fuselage and the wing spars were inserted into the wing connectors. The ball bearings were inserted into the 3D printed supports and the wing connectors. The gear assembly for the flapping mechanism is shown in Figure 17 and the whole assembly can be seen in Figure 18.

5.0 Results and Discussion

5.1 Lift and Thrust Test

In order to validate the lift and thrust results generated from the theoretical calculations, an experimental set up is made. The ornithopter was suspended from the ceiling using threads. A spring balance was attached in both the horizontal axis and vertical axis to measure the force. The least count of the spring balance is 10g. An experimental lift of 2 N and a thrust of 3.2 N is achieved, whereas the theoretical lift at 5 fps is 2.3 N and a thrust of 3.5 N. That gives us an error of 13% for lift and 8.5% for drag.

5.2 Testing of Gears

It is important to check whether the gears are reducing the speed enough we performed a gear test. In this case, the required flaps per second are 7 and it would not be profitable if the reduction is more or less. To check this, a video of the ornithopter was shot at a constant throttle of 50%. Ideally, at 50% throttle, the wings must flap 5 times per second. The video was later slowed down to check if it's giving 25 flaps over a



Figure 19: Snip of flapping video at the lowest position

period of 5s. The results showed that the ornithopter was flapping 24 times over a period of 5s. Figure 19 shows an image of the ornithopter flap testing.

6. Conclusion

The ornithopter is designed considering the mission requirements of achieving flight by flapping its wings and making it look as close to a bird as possible. The aerodynamics of an ornithopter, although very different from a conventional fixed-wing aircraft has few parallels with it. Analyses, both theoretical as well as by simulating the model on software was conducted to make the initial decisions with respect to the design. The ornithopter was manufactured feasibly and the final model weighs around 360g. The wingspan is 1m with a total height of the model at a 45° flapping angle of 0.478m. The average lift produced by the ornithopter is about 4.5N.

References

- [1] A. M. Lippisch, Man powered flight in 1929, *Journal of royal Aeronautical society*, 1960.
- [2] R. T. Jones, Wing Flapping with minimum Energy, *NASA Technical Memorandum*, 1980.
- [3] J. D. DeLaurier, The development of an efficient ornithopter wing, *Aeronautical Journal of the Royal Aeronautical society*, 1993.
- [4] S. Srigrarom and W.-L. Chan, "Ornithopter Type Flapping Wings for Autonomous Micro Air Vehicles," *Aerospace Journal*, 2015.
- [5] M. A. Malik and F. Ahmad, "Effect of Different Design Parameters On Lift, Thrust and Drag of an Ornithopter," in *World Congress on Engineering*, London, UK, 2010.
- [6] J. D. Delaurier and J. Harris, "Experimental study of oscillating wing propulsion," 2012.
- [7] K. Jones and M. Platzer, "Numerical computation of flapping-wing propulsion and power extraction", *AIAA Aerospace Sciences and Exhibit*, 35th, Reno, 1997.
- [8] X. R., "Computational Fluid Dynamics of a Flapping Wing Under Prescribed Motion," 2016.
- [9] J. M. Dietl and E. Garcia†, "Stability in Ornithopter Longitudinal Flight Dynamics," *Journal of Guidance, Control, and Dynamics*, New York, 2008.
- [10] S. J.O., "Experimental and Theoretical Investigation of Large Amplitude Oscillating Foil Propulsion Systems," *Hydronautics Laurel Md*, December 1968.
- [11] G. d. Croon, M. Perçin, B. Remes, R. Ruijsink and D. Wagter, *The DelFly: Design, Aerodynamics and Artificial Intelligence of a Flapping Wing Robot*, Amsterdam: Springer.